

Description and Validation of a Carbon Monoxide and Nitrous Oxide Instrument for High-Altitude Airborne Science (COMA)

5 Emma L. Yates^{1,2}, Levi M. Golston^{1,3}, James R. Podolske¹, Laura T. Iraci¹, Kristen E. Okorn^{1,2,3},
Caroline Dang^{1,2,3}, Roy R. Johnson¹, James Eilers¹, Richard Kolyer¹, Ian Astley^{4,*}, J. Brian Leen^{4,*}

¹NASA Ames Research Center, Moffett Field, CA, USA

²Bay Area Environmental Research Institute, Moffett Field, CA, USA

³NASA Postdoctoral Program, NASA Ames Research Center, Moffett Field, CA, USA

10 ⁴ABB Group, San Jose, CA, USA

*Now at Nikara Labs Inc., Mountain View, CA, USA

Correspondence to: Emma L. Yates (emma.l.yates@nasa.gov)

Abstract. In this work, we describe development of the Carbon monOxide Measurement from Ames (COMA) instrument
15 for measurement of carbon monoxide (CO) and nitrous oxide (N₂O) aboard NASA's WB-57 high altitude research aircraft.
While COMA has previously flown in the cabin of the NASA P-3 platform, here the instrument was modified to operate
in a significantly different environment- an unpressurized pallet flying primarily above 12 km (40,000 ft). Modifications
were made to the laser to allow for detection of CO and N₂O, ruggedization and thermal management were addressed, and
a calibration system was designed to quantify the measurement stability in-flight. Testing was conducted in a thermal
20 vacuum chamber to mimic anticipated ambient conditions experienced inside the WB-57 pallet bay and found electronic
components remained within thermal limits. COMA successfully operated during nine unattended transit flights to and
from South Korea and fifteen research flights during NASA's Asian summer monsoon Chemical & CLimate Project
(ACCLIP) 2022 campaign, which was focused on studying the Asian summer monsoon anticyclone in the Western Pacific.
The CO measurement has an overall uncertainty ranging between 4.1 ppb (at 50 ppb CO) and 5.6 ppb (at 200 ppb CO).
25 N₂O has an overall uncertainty of 2.7 ppb (at 320 ppb N₂O). In addition, COMA observations were compared with two
other in-situ CO instruments co-located on the WB-57: Carbon Monoxide Laser Detector (COLD) 2 and Airborne Carbonic
Oxides and Sulfide Spectrometer (ACOS). Comparisons for 15 flights during the ACCLIP campaign indicate a range in
slope of 1.10–1.15 for COLD2 vs. COMA and 0.94–1.10 for ACOS vs. COMA.

Deleted: 9

1 Introduction

30 The transport of trace gases and aerosols into and within the upper troposphere and lower stratosphere (UTLS) during the
Asian summer monsoon was the focus of the Asian summer monsoon Chemical & CLimate Project (ACCLIP) field

campaign in summer 2022 (Honovich & Pan, 2020; Pan et al., 2025). Carbon monoxide (CO) and nitrous oxide (N₂O) were key measurements during ACCLIP due to their long atmospheric lifetimes. CO is used as a tracer of boundary layer air transport and to infer air mass age (e.g. Pan et al., 2016; Park et al., 2009). Additionally, N₂O is a dominant ozone-depleting substance (Ravishankara et al., 2009) with surface sources and stratospheric loss (Tian et al., 2020), which can indicate in-mixing of aged stratospheric air (e.g., Gonzalez et al., 2021; Hints et al., 1998). As such, understanding the transport mechanisms and behavior of CO and N₂O during the Asian summer monsoon is crucial for evaluating their impact on regional and global climate.

Given its importance, CO has been measured in numerous airborne field campaigns using different aircraft platforms and several different measurement techniques. Established airborne measurements of CO and N₂O with fast instrument response time (seconds) frequently use high-precision infrared (IR) spectroscopic techniques to create spatially and temporally dense datasets. Existing spectroscopic sensor systems operating in the mid-IR use optical sources such as Quantum Cascade Lasers (QCLs) or Interband Cascade Lasers (ICLs) in conjunction with path length enhancement techniques such as multi-pass cells [Gvakharia, Viciani, etc.] or Off-Axis Integrated Cavity Output Spectroscopy (OA-ICOS) [Kloss] (Gvakharia et al., 2018; Kostinek et al., 2019; Pitt et al., 2016; Viciani et al., 2018). Systems operating in the near-IR and utilizing Cavity Ring-Down Spectroscopy (CRDS) have also been fielded (Filges et al., 2015). A detailed overview of these different methods can be found in Zellweger et al. (2012).

This paper describes the work undertaken to convert NASA's Carbon monOxide Measurement from Ames (COMA), a laboratory-based OA-ICOS instrument (Los Gatos Research (now ABB Ltd.)), into an airborne instrument capable of high-altitude (18 km) airborne measurements of CO and N₂O. The airborne operational requirements were that COMA had to operate autonomously in an unpressurized, unheated payload bay of NASA's WB-57 aircraft while flying at altitudes up to 18 km for up to 5 hours of flight time during the ACCLIP campaign. Restrictions on the instrument design included: space/size, low operating pressure (~75 hPa), low in-flight temperature (-20 °C), high pre- and post-flight temperature (>30 °C) and humidity, and requirements for accurate and precise CO and N₂O measurements.

This work details the instrument testing, modifications, and final design of COMA, an instrument designed to meet operational requirements necessary for high altitude flights on NASA's WB-57. We also describe COMA's in-flight performance and operation and briefly discuss observations of CO and N₂O in the UTLS region during the Asian summer monsoon in summer 2022.

2 Instrument Design and Modifications

The operational requirements to fly in one half of a pallet for the payload bay of NASA's WB-57 included instrument size restrictions to physically fit within the space provided, inlet and operating pressure as low as 50 Torr (~75 hPa) when flying at 18 km, low in-flight temperature (-20 °C), but high pre- and post-flight temperature (>30 °C) and humidity during the ACCLIP field campaign. Operation in an unpressurized UTLS environment presents multiple challenges to instrument

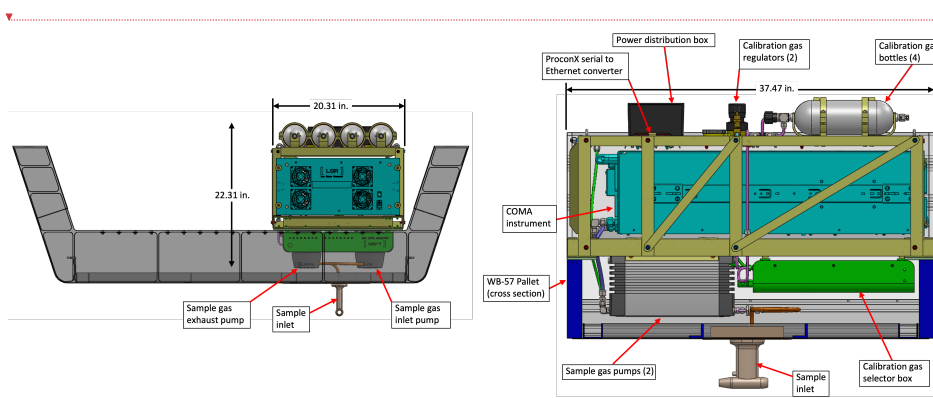
65 stability and performance, since the instrument is designed for ground-based operation. To address these challenges, the
COMA instrument underwent significant modifications, followed by laboratory and environmental chamber testing to
simulate instrument behavior under expected flight conditions.

2.1 Instrument Description

70 COMA is based on a laboratory-oriented OA-ICOS instrument (Los Gatos Research (now ABB Ltd.) GLA251-~~N2OCM~~)
which detects a CO absorption feature as well as nearby N₂O and H₂O absorption features. The original instrument was
manufactured for NASA Ames Research Center in December 2015. The un-modified instrument flew on NASA's P3
aircraft in a 19" rack within the pressurized cabin during the ObserVations of Aerosols above CLouds and their intEractionS
(ORACLES) field campaign in 2018, providing observations of CO and CO₂ on 41 flights up to 7 km altitude (Redemann
et al., 2021).

75 In preparation for ACCLIP, some initial instrument modifications were made, including a computer stack upgrade and
replacing the laser to one with increased sensitivity to CO. Changing the laser allowed for N₂O observations, but at the
expense of removing the CO₂ channel. This was to accommodate the low values of CO expected to be observed in
ACCLIP's UTLS-focused campaign. Other modifications included the installation of higher conductance vacuum control
valves, increasing the measurement range of the sample gas temperature thermistor, and modification of the secondary
80 laser temperature controller setpoint for the expected thermal environment. Sample cell pressure was adjusted to operate at
52.8 torr (70.4 hPa) to accommodate ambient UTLS pressures. Enclosure heaters and two 150 W box fans were added to
the COMA payload to help reduce condensation on the optical windows and to stabilize the COMA enclosure temperature.

2.1.1 Payload Design



85

Deleted: Series

Formatted: Font color: Text 1

Deleted:

Figure 1: COMA payload design (right) and COMA payload installed in NASA's WB-57 payload pallet (looking aft) (left). The engineering drawings show the layout of COMA within NASA's WB-57 payload bay including location of the main COMA instrument (teal) and the two sample pumps (sample gas pumps (2)) the calibration system (four calibration standards (calibration gas bottles (4)) and two regulators (calibration gas regulators (2)) and the MIU (calibration gas selector box)), power distribution box and sample inlet (bottom) and a cross-sectional view of COMA within the permitted envelope, including COMA dimension details (inches) (left).

Deleted: left

Deleted: right)

Formatted: Font: 9 pt, Bold, Font color: Text 1

Formatted: Font color: Text 1

COMA was installed in a pallet for upload into NASA's WB-57 payload bay, as shown in Figure 1. COMA's external mounting structure (chassis) was Alodine treated aluminum and featured side rails to allow for easy installation. The total assembled payload (excluding the pallet) weighed 97.8 kg. The instrument was run from 115 VAC, 60 Hz power from the aircraft. A 28 VDC line for relay activation to power the instrument from the Experimental Control Panel (ECP) was added. The power distribution box contained breakers for the inlet heater, COMA analyzer, commercial multiport inlet unit (MIU), inlet pump, and a master switch. The external pump was controlled by COMA and was the default pump used (COMA switches from operating using an internal to external pump on initial startup). Addition of an 8-channel thermocouple temperature data logger (Madgetech TCTempX8LCD and Type K thermocouples) allowed for measurements of the thermal operating conditions experienced in-flight by COMA as shown in Figure 2.

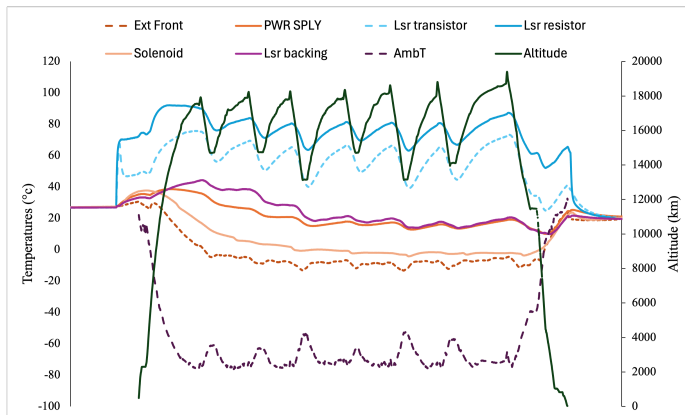
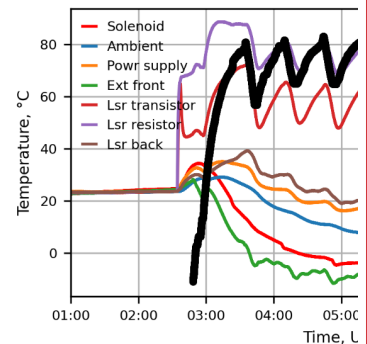


Figure 2: Typical operating thermal conditions experienced by COMA during ACCLIP research flights, data from 21 August 2022 (Research Flight # 11). The black line shows the aircraft altitude (right axis); other lines show measured temperatures at multiple locations inside and outside the COMA chassis. Orange-red (dash) = external front (Ext front), orange = power supply (PWR SPLY), light blue (dash) = laser transistor (Lsr transistor), blue = laser resistor (Lsr resistor), light orange = solenoid, purple = laser backing, purple (dash) = ambient temperature (Amb T).

Deleted: An in-flight calibration system was designed and implemented as described in Section 2.1.2.



Deleted:

Deleted: heavy

Deleted: Red = solenoid temperature, blue = ambient temperature, orange = temperature of the power supply, green = external side, dark red = laser transistor temperature, purple = laser resistor temperature, brown = laser backing temperature, black = environmental chamber pressure altitude.

2.1.2 Flow System

COMA used an inlet probe, which has previously flown on NASA's WB-57, from NASA Goddard Space Flight Center known as the "CAFE Inlet" (St. Clair et al., 2019) mounted on the underside of the pallet. The inlet includes a cartridge heater (SunRod) controlled to 30 °C by a proportional controller (Minco CT335). Inside the payload bay, Teflon FEP or stainless-steel tubing carries the sample flow from the inlet to the instrument via an inlet diaphragm pump (KNF Group, NF N90 APE-W), relief valve (TAVCO 20 psia), and high-flow solenoid valve. The solenoid valve directs the sample air to one of the eight available ports on the MIU, which is programmed to control COMA's air sampling and calibration sampling pattern (discussed in Section 4.3). The inlet diaphragm pump, along with an internal (to COMA) pump and the external (to COMA) exhaust pump (KNF Group, NF N90 APE-W) pull the sample through COMA and exhaust it to the ambient atmosphere. COMA contains internal valves that maintain a pressure of 52.8 Torr within COMA's sampling cell.

Formatted: Highlight

A diagram of COMA's flow system is shown in Figure 3.

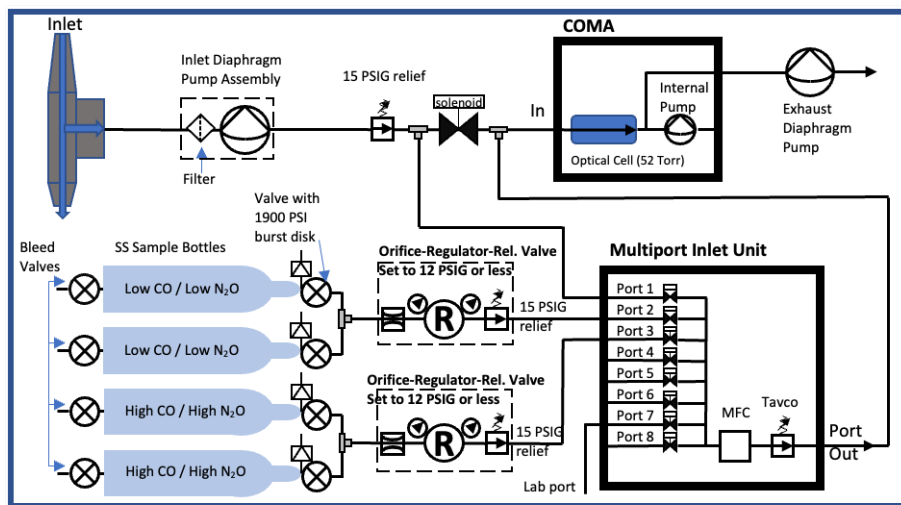


Figure 3: COMA flow diagram.

COMA's in-flight calibration system consisted of four Swagelok double-ended stainless steel cylinders (304L-HDF4-1000) with 1800 PSI maximum allowable working pressure (MAWP) and 1000 PSIG maximum operating pressure (MOP). Prior to the ACCLIP campaign deployment, the in-flight cylinders were filled from one of four source cylinders: two primary NOAA Global Monitoring Laboratory whole air standards, certified by the WMO Central Calibration Laboratory for CO and N₂O (low CO standard "NOAA 1", (tank # CC745344, CO ~51.77 ppb ±0.94, N₂O ~265.89 ppb ±0.03 and high CO

Deleted: During

Deleted:

Deleted: ERSL

standard “NOAA 2”, (tank # CC746190, CO ~164.34 ppb ±1.84, N₂O~348.06 ppb ±0.05), and two secondary standards (“Matheson 1”, ~200 ppb each of CO and N₂O, and “Matheson 2”, ~1000 ppb each of CO and N₂O). The NOAA standards are referenced on the WMO CO_X2014A scale for CO and the NOAA-2006A scale for N₂O. Further details on the calibration scales can be found at <https://gml.noaa.gov/ccl/refgas.html>. Only two standard cylinders were open at any one time (the other two had valve locks installed on the unopened cylinders to prevent leakage). The two NOAA-filled cylinders were the first to be sampled by COMA during in-flight calibrations before moving on to sample the secondary standards, these standards were deployed during the field campaign which allowed the in-flight calibration system to be re-filled the secondary standards (but not with the primary).

Deleted: as well as

Deleted: <https://gml.noaa.gov/ccl/refgas.html>

Deleted:

Formatted: Font color: Text 1

Formatted: Font color: Text 1

Deleted:

Deleted:

Deleted:

2.1.3 Telemetry

COMA was required to run autonomously onboard the WB-57. The instrument could be controlled (on/off) by the Science Equipment Operator located in the rear cockpit to power cycle the instrument. Bandwidth to communicate with the instrument in-flight was limited. To address this, we developed a communication and processing software for real-time monitoring on the ground, consisting of a Python script which ran on the analyzer to access data files in 1 Hz output user data protocol (UDP) packets. It also included a proconX SERIP-100 serial-to-ethernet converter as backup system, which sent UDP packets for real time monitoring on the ground. In addition, NASA’s Mission Tools Suite (MTS) was used to communicate to the ground while in-flight (<https://airbornescience.nasa.gov/tracker/>).

2.2 Instrument Performance

2.2.1 Environmental Chamber Testing

Prior to deployment, COMA was extensively tested in the NASA Ames Research Center Engineering Evaluation Laboratory (EEL). The environmental chamber testing plans centered around two main concerns. First, the thermal limits of the instrument’s components were tested to ensure safe operation of the laser and other components under UTLS-like conditions. Second, the stability of the instrument was tested by sampling from a standard gas mixture while simulating UTLS conditions.

In the environmental chamber, seven thermocouples were placed inside the COMA instrument, one along the middle dividing panel inside sensor (Figure 4: mid-rib), and at six locations considered critical or at risk of overheating. Figure 4 shows the thermal performance of COMA’s individual components during a simulated UTLS flight, when the chamber altitude (pressure) was varied (Figure 4: black line, secondary y-axis). Results from the thermal testing showed that at altitudes up to 18 km, components did not overheat noticeably outside of their operational ranges.

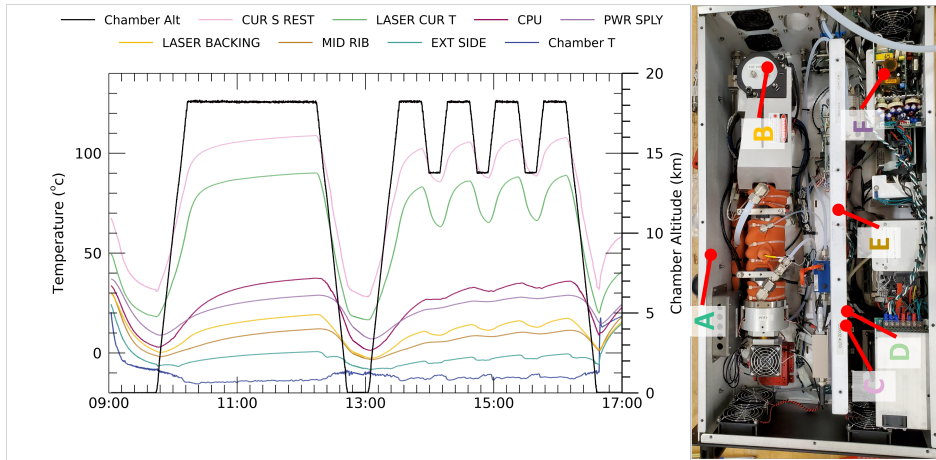
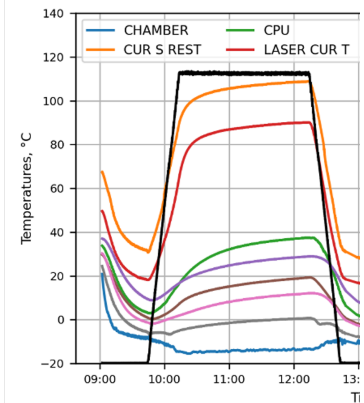


Figure 4: Environmental chamber timeseries showing COMA's component temperatures during a simulated UTLS flight conducted on 20 May 2022 (right). Corresponding thermocouple locations are shown on the right: external side = EXT SIDE (A), laser backing (B), laser current sensing resistor = CUR S REST (C), laser current temperature = LASER CUR T (D), internal dividing panel = MID-RIB (E), and power supply = PWR SPLY (F).

Allan deviation (Allan, 1987) was used as a metric of COMA's stability as shown in Figure 5, which presents the Allan deviation as a function of averaging time to illustrate how precision changes based on data averaging. The results show a laboratory 1 Hz precision of ~0.13 ppb for CO and ~0.19 ppb for N₂O. Precision improves with increased data averaging during standard sampling in the laboratory (blue) up to ~1000 s, after which additional time averaging has little benefit. In the environmental chamber, under conditions shown in Figure 4, precision is similar at 1 Hz and improves with increased averaging at approximately the same rate of change as in the laboratory up to 10 s, after which the improvements in precision are at a slower rate of change, likely due to noise or additional uncertainty in the measurements due to changing operational (chamber temperature and pressure) conditions.



Deleted:

Formatted: Font color: Text 1

Deleted: Black = chamber altitude, blue = chamber temperature, purple = power supply (PWR SPLY, letter F), pink = internal dividing panel (MID-RIB, letter E), orange = laser current sensing resistor (CUR S REST, letter C), red = laser current temperature (LASER CUR T, letter D),

Deleted: brown = laser backing (letter B), and grey =

Deleted: (

Deleted: ,

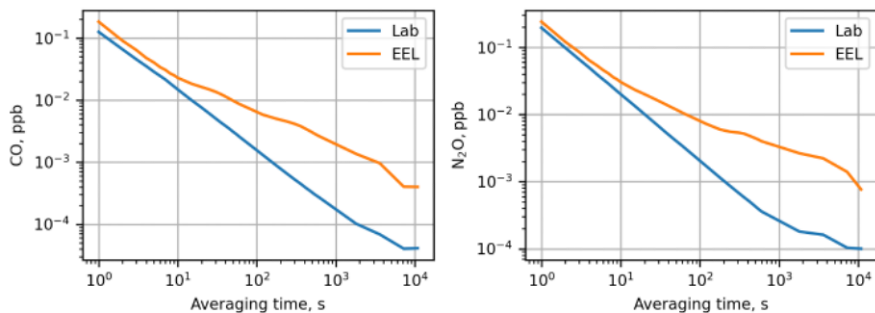
Deleted: letter

Deleted:)

Deleted: of COMA instrument (left).

Formatted: Line spacing: single

Deleted: from the Allan deviations



205 Figure 5. Allan deviation results, comparing data collected in lab (blue) and an environmental chamber (EEL, orange) during standard sampling for CO (left) and N₂O (right). Under both conditions, 1 Hz precision ~ 0.1 – 0.2 ppb for both gases. See Figure 4 for chamber pressure and temperature details.

2.2.2 Instrument Linearity

210 Linearity assessments were performed using a flow mixing system equipped with high accuracy mass flow controllers (Alicat Scientific Inc., MC-1SLP-D, (most recent calibration, reported accuracy was ±0.6 % of reading (3 Nov 2021)), and OMEGA Engineering inc., FMA-2602A, (most recent calibration, reported accuracy was ±0.4 % of reading (11 Jul 2021)). A secondary synthetic CO standard (~1000 ppb each of CO and N₂O) and a zero-air standard were used to perform the linearity mixing analysis. The linearity assessment for COMA is shown in Figure 6 and demonstrates that COMA is highly linear over a wide range of CO and N₂O mixing ratios. Figure 6 shows COMA to be linear (slope of 1.00) to within 0.1% between 25-1000 ppb CO and linear (slope of 1.00) within 0.1% between 25-850 ppb N₂O.

Formatted: Line spacing: 1.5 lines, Adjust space between Latin and Asian text, Adjust space between Asian text and numbers

Deleted:

Deleted: .

Formatted: Font: (Default) Times New Roman

Formatted: Font: (Default) Times New Roman

Formatted: Font: (Default) Times New Roman

Formatted: Font: (Default) Times New Roman, Subscript

Formatted: Font: (Default) Times New Roman

Formatted: Font: (Default) Times New Roman, Font color: Text 1

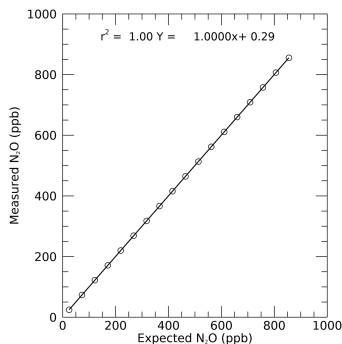
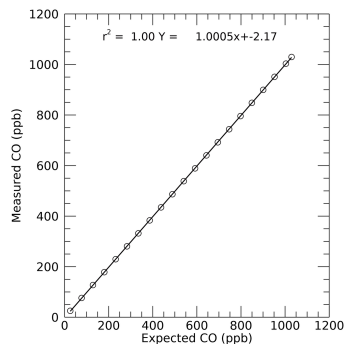


Figure 6: COMA Instrument linearity for CO (left) and N₂O (right) as performed under laboratory conditions on 20 October 2023.

Formatted: Font color: Red

2.2.3 Instrument Calibration and Measurement Uncertainty

Calibration to NOAA standards was applied (see Section 2.1.2) using data collected at ground level throughout the campaign as well as after to help account for time drift in the instrument. Outliers, which deviated from the mean by more than 4 standard deviations were removed. Multivariate linear regressions with time and measured concentration as dependent variables were applied for both CO and N₂O. Slight degradation in instrument response was observed over the course of the campaign and was accounted for with the inclusion of an elapsed time term in the final calibrations. The estimation of overall accuracy of CO includes small contributions due to accuracy of the standard gases but was dominated by the residuals remaining after this calibration to NOAA standards. Overall accuracy for CO was determined to be ± 3.8 ppb over the calibration range. Accuracy for N₂O is comprised equally of the contributions from the residuals after calibration to NOAA standards (1.0 ppb) and NOAA scale uncertainty (0.31 %). Given the relatively small range of N₂O values observed in the field, overall accuracy in N₂O can be approximated by the value of +/- 1.4 ppb, as calculated at N₂O = 320 ppb.

Formatted: Space Before: 0 pt, After: 0 pt

Deleted: which deviated

Formatted: Font color: Text 1

Formatted: Font: (Default) Times New Roman, Not Italic

Formatted: Font: (Default) Times New Roman

Deleted: terms

Formatted: Font color: Text 1

The in-flight calibration system ran a cycle of 60 s of low-mixing ratio calibration gas, followed by 60 s of high mixing ratio gas periodically throughout each flight. Figure 7 shows the results from in-flight calibrations for CO (bottom) and N₂O (top) during the ACCLIP deployment for primary whole air NOAA standards (left) and secondary synthetic standards (right). Note that only the NOAA standards were used for linear calibration fits; the secondary synthetic standards were only used for internal assessment. The intra- and inter-flight variability among flight calibrations give an indication of the in-flight instrument 1σ precision. The standard deviations of observations at three different mixing ratios were seen to vary slightly with mixing ratio as shown in Equation 1 and Equation 2. For example, At 320 ppb N₂O, precision = 2.3 ppb (equivalent to 0.7 %). At 50 ppb CO, precision = 1.4 ppb (equivalent to 2.8 %), while at 200 ppb CO, precision = 4.1 ppb (equivalent to 2.1 %).

Deleted: ,

Deleted: ,

Deleted: ,

$$\text{CO precision} = 1.79 \times 10^{-02} \times \text{CO (ppb)} + 0.50 \quad \text{Equation 1}$$

$$\text{N}_2\text{O precision} = 8.05 \times 10^{-03} \times \text{N}_2\text{O (ppb)} - 0.25 \quad \text{Equation 2}$$

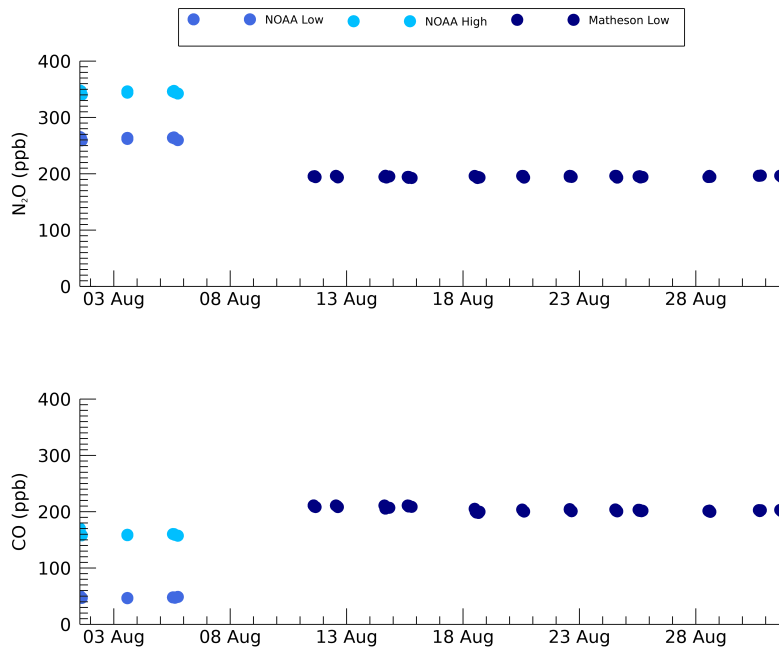
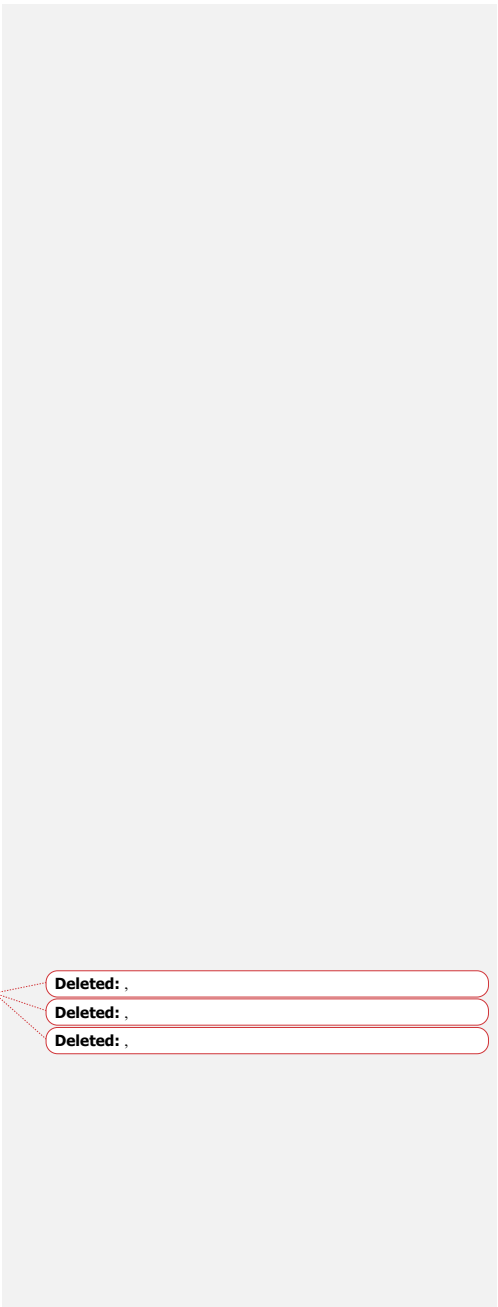


Figure 7: Mean value from individual in-flight calibration periods for CO (bottom) and N₂O (top) during the ACCLIP deployment for primary whole air NOAA standards (prior to August 8, 2022) and secondary Matheson synthetic standards (after August 11, 2022). The standard deviation of each calibration mean value is significantly smaller than the size of the symbol plotted. Note, the in-flight calibration system was filled prior to deployment to last the duration of the ACCLIP field campaign. The primary whole air standards were sampled first during in-flight calibrations (prior to August 8, 2022), once these were exhausted, the secondary standards were used for in-flight calibrations (on/after August 11, 2022), hence the switch between calibration standards.

255 Overall uncertainty is determined by the square root of the sum of the squares of the accuracy and precision terms. If
 260 desired, total uncertainty for each measurement can be calculated from individual terms. Under flight conditions at 320 ppb
 N₂O, total uncertainty is 2.7 ppb. At 50 ppb CO, total uncertainty is 4.1 ppb; at 200 ppb CO total uncertainty is 5.6 ppb.

2.2.4 Data Processing

In addition to applying the calibration equations described in Section 2.2.3, several steps were taken to ensure the quality
 265 of the reported atmospheric observations of CO and N₂O. Measurements recorded during periodic calibration cycles and
 up to a minute of data before and after were removed, as were measurements before and during take-off and after landing.



Deleted: ,
 Deleted: ,
 Deleted: ,

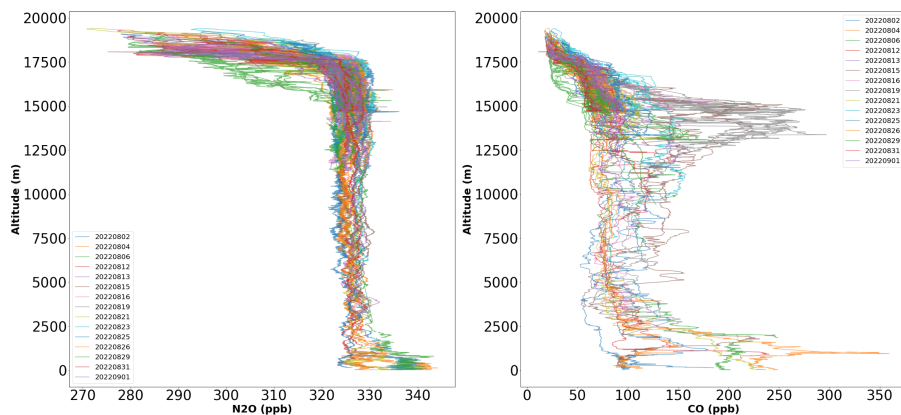
270 A time lag is present in the raw data due to combination of physical effects and clock offsets, which were accounted for by determining a median offset for each flight by correlation to an additional CO instrument (COLD2) onboard the WB-57. When COMA's measurement cell pressure deviated from the median pressure by more than 0.25%, N₂O data were omitted, and CO data were omitted on a case-by-case basis. (CO measurements were more robust against cell pressure oscillations, but not immune.) Additional deviations from nominal operating conditions were evaluated on a case-by-case basis.

275 3 COMA In-flight Data

COMA flew onboard NASA's WB-57 on four test flights (TF) from Ellington Field, TX in summer 2021, one functional check flight and two test flights in Ellington Field, TX in July 2022, five outbound transit flights from Ellington Field, TX, USA to Osan Air Base, South Korea, 15 research flights (RF) from Osan Air Base and four return transit flights to Ellington Field, TX, USA. Data is archived and publicly available at the NASA Langley Research Center (LaRC) Distributed Active

280 Archive Center (DAAC) (<https://www-air.larc.nasa.gov/cgi-bin/ArcView/acclip.2022>).

The WB-57 typically profiled multiple times through the UTLS during each research flight, resulting in vertical profiles of CO and N₂O. Figure 7 shows a summary of observations of N₂O and CO reported by COMA plotted by altitude and colored by flight date for ACCLIP campaign research flights from Osan, South Korea. General observations include day-to-day variability in CO and N₂O within the boundary layer (<~2 km). Within the free-troposphere (~2.5 to 12.5 km) N₂O is well-mixed, with little day-to-day variability, however there is more variability observed in CO. The UTLS region (~12.5 to 16 km), shows highly variable CO, with the interception of lofted pollution originating from convective influences over Asia during different flights. In contrast, N₂O remains well-mixed in this altitude region. Decreasing profiles of both CO and N₂O were observed within the stratosphere (>~16 km).



Deleted: from COMA

Deleted: ,

Deleted: research

Figure 8: Vertical profiles of all N₂O (left) and CO (right) measurements taken by COMA during the ACCLIP campaign research flights from Osan, Korea in July and August 2022.

295 **3.1 Data Comparison with COLD2 and ACOS**

During the ACCLIP campaign, two other instruments were onboard NASA's WB-57 that measured CO: Carbon Monoxide Laser Detector (COLD) 2 and Airborne Carbonic Oxides and Sulfide Spectrometer (ACOS). COLD2, operated by CNR-INO (CNR National Institute of Optics), is a mid-infrared quantum cascade laser spectrometer that has previously flown on an M55 aircraft during StratoClim (Stratospheric and upper tropospheric processes for better climate predictions) (Viciani et al., 2018). ACOS is a NOAA-operated, Off-Axis Integrated Cavity Output Spectrometer (ICOS) that measures carbonyl sulfide (OCS) and CO (Gurganus et al., 2024).

Figure 9 shows the CO data comparison as a linear regression and demonstrates an excellent overall agreement between the three CO instruments. The cross plot shows the correlation of the 1 Hz CO measurements with ACOS and COLD2 CO plotted on the vertical axis and COMA CO on the horizontal axis, with a slope of 1.06 for COLD2 ($r^2 = 0.99$) and 1.01 for ACOS ($r^2 = 0.98$), indicating strong agreement throughout the ACCLIP field campaign.

305 ACOS ($r^2 = 0.98$), indicating strong agreement throughout the ACCLIP field campaign.

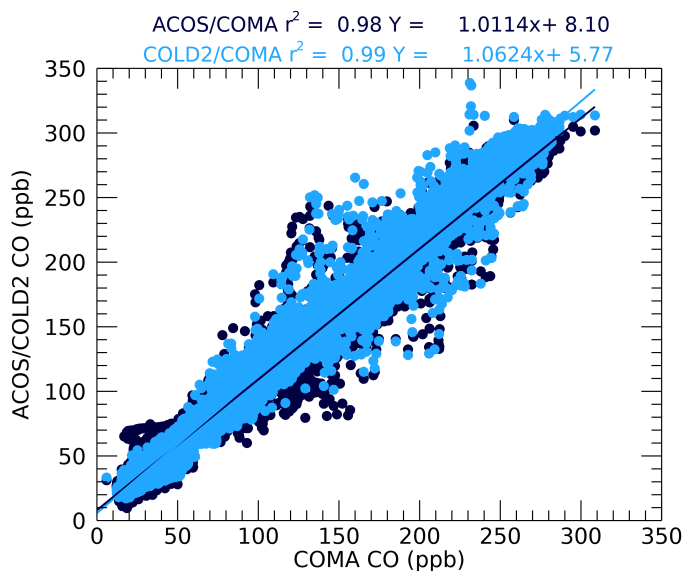


Figure 9: Linear regression of ACOS and COLD2 vs COMA for all 15 ACCLIP science flights.

Deleted: is

Deleted: operated

Deleted: a

Deleted: n

Deleted: both (a) a time series along with altitude for ACCLIP flight on 29th August 2022 and (b) a cross plot with

Deleted: . Figure 9

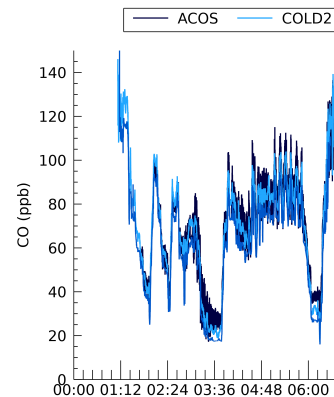
Deleted: 1.1

Deleted: 8

Deleted:

Deleted: 6

Deleted: on 29th August 2022. Comparisons for 15 flights from the campaign indicate a range in slope of 1.10–1.15 for COLD2 and 0.94–1.10 for ACOS



Deleted:

Deleted: Time series of CO data from COMA (medium blue), COLD2 (light blue) and ACOS (navy blue) (left

Deleted:) and l

Deleted: (right) on 29th August 2022 (time in UTC).

4 Conclusion

330 The NASA COMA instrument provides high-sensitivity measurements of CO and N₂O from ground-level to an altitude of ~18 km. COMA flew onboard NASA's WB-57 during 24 flights, supporting the ACCLIP field campaign based in Korea during 2022. COMA data from this campaign is archived and publicly available (<https://www-air.larc.nasa.gov/cgi-bin/ArcView/acclip.2022>).

335 During ACCLIP, COMA flew primarily between 12 and 19 km within an unpressurized pallet of the WB-57. To operate successfully in these conditions, significant modifications were made to the original laboratory-oriented instrument, followed by laboratory and environmental chamber testing to simulate instrument behavior under expected flight conditions.

340 This paper details the COMA design modifications, including the installation into the WB-57 payload pallet required for flight. Details of internal instrument modifications and changes to operational parameters are detailed in Section 2. External modifications to COMA to accommodate flights in the UTLS region included additional heaters and fans to help reduce condensation and for thermal management. An in-flight calibration system was added to the COMA payload to allow an evaluation of COMA in-flight performance, and an MIU to allow gas sampling selection (e.g. inlet, calibration standard, detailed in Section 2.1.2).

345 COMA instrument performance was assessed through extensive laboratory and environmental chamber testing (detailed in Section 2.2). This testing included assessments of COMA operation under simulated UTLS conditions, linearity assessment, assessment of laboratory and in-flight COMA calibrations, and data comparison of COMA to two independent instruments measuring CO (COLD2 and ACOS). Overall, the instrument achieved an uncertainty during ACCLIP of 2.7 ppb N₂O (at 320 ppb) and 5.6 ppb CO (at 200 ppb). COMA's successful integration aboard NASA's WB-57, demonstrated field performance, and favorable comparison to other independent instruments enable a new CO and N₂O capability for airborne science measurements in the upper troposphere and lower stratosphere.

350 *Author contributions:* JRP and LTI supervised the project. JE, RRJ, and JRP led design and integration onto the WB-57 aircraft. JBL, IA, JRP, and RRJ contributed towards environmental chamber testing and system design. LMG, JRP, RRJ, RK, LTI, KEO, CD, and ELY were involved in lab and field investigation. KEO, JRP, and LMG curated the COMA data, KEO and LMG wrote software used. LMG and ELY wrote the original draft, which was revised with feedback from all
355 authors.

Competing interests: The authors declare that they have no conflict of interest.

Deleted: The NASA COMA instrument provides high-sensitivity measurements of CO and N₂O from ground-level to an altitude of ~18 km. COMA flew onboard NASA's WB-57 during 24 flights, supporting the ACCLIP field campaign based in Korea during 2022. COMA flew primarily between 12 and 19 km. The instrument achieved an overall uncertainty of 2.7 ppb N₂O (at 320 ppb) and 5.6 ppb CO (at 200 ppb). COMA's successful integration aboard NASA's WB-57, demonstrated field performance, and favorable comparison to other independent instruments enable a new CO and N₂O capability for airborne science measurements in the upper troposphere and lower stratosphere.[†]

Code and data availability: Final ACCLIP campaign data is publicly archived on <https://www-air.larc.nasa.gov/cgi-bin/ArcView/acclip.2022>. Additional data can be made available by the corresponding author. Code used in the manuscript will be available on <https://github.com/KristenOkoni/COMA>.

Deleted: ,

Deleted: orientated

Deleted:

Deleted: ,

Acknowledgements

The COMA team was supported by the NASA Earth Science Research and Analysis Program (K. Jucks, J. Kaye), the
380 NASA Postdoctoral Program, and NASA Ames Internal Research and Development funding. Technical contributions from
Bob Provencal at ABB, Chris Wilson at NASA Ames and staff at the Ames Engineering Evaluation Laboratory (EEL) are
greatly appreciated. We gratefully recognize the efforts of all involved in the ACCLIP mission, from inception to project
management to aircraft support and beyond. This work benefits from COLD2 data provided by Francesco D'Amato, Silvia
Viciani and Giovanni Bianchini at CNR-INO. The COLD2 team was supported by ESA, within the frame of Project
385 SVANTE-QA4EO. The ACOS data provided by Colin Gurganus at NOAA CSL was supported by the NOAA Chemical
Sciences Laboratory and the University of Colorado through the Cooperative Institute for Earth System Research and Data
Science (CIESRDS).

Deleted: from

Deleted: Silvia

Deleted: The

Deleted: data

Deleted: by

Deleted: Colin

Deleted: NOAA

References

- Allan, D. W.: Should the Classical Variance be Used as a Basic Measure in Standards Metrology?, IEEE Transactions on
390 Instrumentation and Measurement, vol. IM-36, no. 2, pp. 646–654, June 1987, doi: 10.1109/TIM.1987.6312761,
1987.
- Baer, D. S., Paul, J. B., Gupta, M., and O'Keefe, A.: Sensitive absorption measurements in the near-infrared region using
off-axis integrated-cavity-output spectroscopy, Appl. Phys. B Lasers Opt., 75, 261–265,
https://doi.org/10.1007/s00340-002-0971-z, 2002.
- 395 Barret, B., Sauvage, B., Bennouna, Y., and Le Flochmoen, E.: Upper-tropospheric CO and O₃ budget during the Asian
summer monsoon, Atmospheric Chem. Phys., 16, 9129–9147, https://doi.org/10.5194/acp-16-9129-2016, 2016.
- Barrett, P. A., Abel, S. J., Coe, H., Crawford, I., Dobracki, A., Haywood, J., Howell, S., Jones, A., Langridge, J.,
McFarquhar, G. M., Nott, G. J., Price, H., Redemann, J., Shinozuka, Y., Szpek, K., Taylor, J. W., Wood, R., Wu, H.,
Zuidema, P., Bauguitte, S., Bennett, R., Bower, K., Chen, H., Cochrane, S., Cotterell, M., Davies, N., Delene, D.,
400 Flynn, C., Freedman, A., Freitag, S., Gupta, S., Noone, D., Onasch, T. B., Podolske, J., Poellot, M. R., Schmidt, S.,
Springston, S., Sedlacek III, A. J., Trembath, J., Vance, A., Zawadowicz, M. A., and Zhang, J.: Intercomparison of
airborne and surface-based measurements during the CLARIFY, ORACLES and LASIC field experiments,
Atmospheric Meas. Tech., 15, 6329–6371, https://doi.org/10.5194/amt-15-6329-2022, 2022.
- Bernath, P. F., Yousefi, M., Buzan, E., and Boone, C. D.: A Near-Global Atmospheric Distribution of N₂O Isotopologues:
405 N₂O Isotopologues, Geophys. Res. Lett., 44, 10,735–10,743, https://doi.org/10.1002/2017GL075122, 2017.
- Bourgeois, I., Peischl, J., Neuman, J. A., Brown, S. S., Allen, H. M., Campuzano-Jost, P., Coggon, M. M., DiGangi, J. P.,
Diskin, G. S., Gilman, J. B., Gkatzelis, G. I., Guo, H., Halliday, H. A., Hanisco, T. F., Holmes, C. D., Huey, L. G.,
Jimenez, J. L., Lamplugh, A. D., Lee, Y. R., Lindaas, J., Moore, R. H., Nault, B. A., Nowak, J. B., Pagonis, D.,
Rickly, P. S., Robinson, M. A., Rollins, A. W., Selimovic, V., St. Clair, J. M., Tanner, D., Vasquez, K. T., Veres, P.

- R., Warneke, C., Wennberg, P. O., Washenfelder, R. A., Wiggins, E. B., Womack, C. C., Xu, L., Zarzana, K. J., and Ryerson, T. B.: Comparison of airborne measurements of NO, NO₂, HONO, NO_y, and CO during FIREX-AQ, *Atmospheric Meas. Tech.*, 15, 4901–4930, <https://doi.org/10.5194/amt-15-4901-2022>, 2022.
- 420 Diskin, G. S., Podolske, J. R., Sachse, G. W., and Slate, T. A.: Open-path airborne tunable diode laser hygrometer, *International Symposium on Optical Science and Technology*, Seattle, WA, 4817, 196–204, <https://doi.org/10.1117/12.453736>, 2002.
- Filges, A., Gerbig, C., Chen, H., Franke, H., Klaus, C., and Jordan, A.: The IAGOS-core greenhouse gas package: a measurement system for continuous airborne observations of CO₂, CH₄, H₂O and CO, *Tellus B Chem. Phys. Meteorol.*, 67, 27989–28008, <https://doi.org/10.3402/tellusb.v67.27989>, 2015.
- 425 Gomez-Pelaez, A. J., Ramos, R., Cuevas, E., Gomez-Trueba, V., and Reyes, E.: Atmospheric CO₂, CH₄, and CO with the CRDS technique at the Izaña Global GAW station: instrumental tests, developments, and first measurement results, *Atmospheric Meas. Tech.*, 12, 2043–2066, <https://doi.org/10.5194/amt-12-2043-2019>, 2019.
- Gonzalez, Y., Commane, R., Manninen, E., Daube, B. C., Schiferl, L. D., McManus, J. B., McKain, K., Hints, E. J., 430 Elkins, J. W., Montzka, S. A., Sweeney, C., Moore, F., Jimenez, J. L., Campuzano Jost, P., Ryerson, T. B., Bourgeois, I., Peischl, J., Thompson, C. R., Ray, E., Wennberg, P. O., Crounse, J., Kim, M., Allen, H. M., Newman, P. A., Stephens, B. B., Apel, E. C., Hornbrook, R. S., Nault, B. A., Morgan, E., and Wofsy, S. C.: Impact of stratospheric air and surface emissions on tropospheric nitrous oxide during ATom, *Atmos. Chem. Phys.*, 21, 11113–11132, <https://doi.org/10.5194/acp-21-11113-2021>, 2021.
- 435 Gottschaldt, K.-D., Schlager, H., Baumann, R., Bozem, H., Eyring, V., Hoor, P., Jöckel, P., Jurkat, T., Voigt, C., Zahn, A., and Ziereis, H.: Trace gas composition in the Asian summer monsoon anticyclone: a case study based on aircraft observations and model simulations, *Atmospheric Chem. Phys.*, 17, 6091–6111, <https://doi.org/10.5194/acp-17-6091-2017>, 2017.
- Gurganus, C., Rollins, A. W., Waxman, E., Pan, L. L., Smith, W. P., Ueyama, R., Feng, W., Chipperfield, M. P., Atlas, E. 440 L., Schwarz, J. P., Lee, S., Thornberry, T. D.: Highlighting the impact of anthropogenic OCS emissions on the stratospheric budget with in-situ observations, *ESS Open Archive*, doi: 10.22541/essoar.172801406.62154439/v1, 2024.
- Gvakharia, A., Kort, E. A., Smith, M. L., and Conley, S.: Testing and evaluation of a new airborne system for continuous N₂O, CO₂, CO, and H₂O measurements: the Frequent Calibration High-performance Airborne Observation System (FCHAOS), *Atmospheric Meas. Tech.*, 11, 6059–6074, doi: 10.5194/amt-11-6059-2018, 2018.
- 445 Hints, E., Boering, K. A., Weinstock, E. M., Anderson, J. G., Gary, B. L., Pfister, L., Daube, B. C., Wofsy, S. C., Loewenstein, M., Podolske, J. R., Margitan, J. J., and Bu, T. T.: Troposphere-to stratosphere transport in the lowermost stratosphere from measurements of H₂O, CO, N₂O and O₃, *Geophys. Res. Lett.*, 25, 14, 2655–2658, <https://doi.org/10.1029/98GL01797>, 1998.

- 450 Honomichl, S. B., and Pan, L. L.: Transport from the Asian Summer Monsoon Anticyclone Over the Western Pacific, *J. Geophys. Res.*, 125, e2019JD032094, <https://doi.org/10.1029/2019JD032094>, 2020.
- Kostinek, J., Roiger, A., Davis, K. J., Sweeney, C., DiGangi, J. P., Choi, Y., Baier, B., Hase, F., Groß, J., Eckl, M., Klausner, T., Butz, A.: Adaptation and performance assessment of a quantum and interband cascade laser spectrometer for simultaneous airborne in situ observation of CH₄, C₂H₆, CO₂, CO and N₂O, *Atmospheric Measurement Techniques*, 12, 1767-1783, doi: 10.5194/amt-12-1767-2019, 2019.
- 455 Kloss, C., Tan, V., Leen, J. B., Madsen, G. L., Gardner, A., Du, X., Kulesa, T., Schillings, J., Schneider, H., Schrade, S., Qiu, C., and von Hobe, M.: Airborne Mid-Infrared Cavity enhanced Absorption spectrometer (AMICA), *Atmospheric Meas. Tech.*, 14, 5271–5297, <https://doi.org/10.5194/amt-14-5271-2021>, 2021.
- Nédélec, P., Cammas, J.-P., Thouret, V., Athier, G., Cousin, J.-M., Legrand, C., Abonnel, C., Lecoeur, F., Cayez, G., and Marizy, C.: An improved infrared carbon monoxide analyser for routine measurements aboard commercial Airbus aircraft: technical validation and first scientific results of the MOZAIC III programme, *Atmospheric Chem. Phys.*, 3, 1551–1564, <https://doi.org/10.5194/acp-3-1551-2003>, 2003.
- 460 Nédélec, P., Blot, R., Boulanger, D., Athier, G., Cousin, J.-M., Gautron, B., Petzold, A., Volz-Thomas, A., and Thouret, V.: Instrumentation on commercial aircraft for monitoring the atmospheric composition on a global scale: the IAGOS system, technical overview of ozone and carbon monoxide measurements, *Tellus B Chem. Phys. Meteorol.*, 67, 27791–27808, <https://doi.org/10.3402/tellusb.v67.27791>, 2015.
- 465 Novelli, P. C.: CO in the atmosphere: measurement techniques and related issues, *Chemosphere - Glob. Change Sci.*, 1, 115–126, [https://doi.org/10.1016/S1465-9972\(99\)00013-6](https://doi.org/10.1016/S1465-9972(99)00013-6), 1999.
- Pan, L. L., Honomichl, S. B., Kinnison, D. E., Abalos, M., Randel, W. J., Bergman, J. W., and Bian, J.: Transport of chemical tracers from the boundary layer to stratosphere associated with the dynamics of the Asian summer monsoon, *J. Geophys. Res. Atmospheres*, 121, 14, 159-174, <https://doi.org/10.1002/2016JD025616>, 2016.
- Pan, L. L.: The Asian Summer Monsoon Chemical and Climate Impacts Project (ACCLIP): An Overview, in preparation (submission intended in March 2025).
- Park, M., Randel, W. J., Emmons, L. K., Bernath, P. F., Walker, K. A., and Boone, C. D.: Chemical isolation in the Asian monsoon anticyclone observed in Atmospheric Chemistry Experiment (ACE-FTS) data, *Atmospheric Chem. Phys.*, 8, 757–764, <https://doi.org/10.5194/acp-8-757-2008>, 2008.
- 475 Park, M., Randel, W. J., Emmons, L. K., and Livesey, N. J.: Transport pathways of carbon monoxide in the Asian summer monsoon diagnosed from Model of Ozone and Related Tracers (MOZART), *J. Geophys. Res.* 114, D08303, <https://doi.org/10.1029/2008JD010621>, 2009.
- 480 Paul, J. B., Lapson, L., and Anderson, J. G.: Ultrasensitive absorption spectroscopy with a high-finesse optical cavity and off-axis alignment, *Appl. Opt.*, 40, 4904–4910, <https://doi.org/10.1364/AO.40.004904>, 2001.
- Pitt, J. R., Le Breton, M., Allen, G., Percival, C. J., Gallagher, M. W., Bauguitte, S. J.-B., O’Shea, S. J., Muller, J. B. A., Zahniser, M. S., Pyle, J., and Palmer, P. I.: The development and evaluation of airborne in situ N₂O and CH₄ sampling

- using a quantum cascade laser absorption spectrometer (QCLAS), *Atmospheric Meas. Tech.*, 9, 63–77, 485 <https://doi.org/10.5194/amt-9-63-2016>, 2016.
- Provencal, R., Gupta, M., Owano, T. G., Baer, D. S., Ricci, K. N., O’Keefe, A., and Podolske, J. R.: Cavity-enhanced quantum-cascade laser-based instrument for carbon monoxide measurements, *Appl. Opt.*, 44, 6712–6717, <https://doi.org/10.1364/AO.44.006712>, 2005.
- Ravishkara, A. R., Daniel, J. S., Portmann R. W.: Nitrous Oxide (N₂O): The Dominant Ozone-Depleting Substance Emitted 490 in the 21st Century, *Science*, 326, 5929, 123–125, doi: 10.1126/science.1176985, 2009.
- Redemann, J., Wood, R., Zuidema, P., Doherty, S. J., Luna, B., LeBlanc, S. E., Diamond, M. S., Shinozuka, Y., Chang, I. Y., Ueyama, R., Pfister, L., Ryoo, J.-M., Dobracki, A. N., da Silva, A. M., Longo, K. M., Kacenelenbogen, M. S., Flynn, C. J., Pistone, K., Knox, N. M., Piketh, S. J., Haywood, J. M., Formenti, P., Mallet, M., Stier, P., Ackerman, A. S., Bauer, S. E., Fridlind, A. M., Carmichael, G. R., Saide, P. E., Ferrada, G. A., Howell, S. G., Freitag, S., Cairns, 495 B., Holben, B. N., Knobelspiesse, K. D., Tanelli, S., L’Ecuyer, T. S., Dzambo, A. M., Sy, O. O., McFarquhar, G. M., Poellot, M. R., Gupta, S., O’Brien, J. R., Nenes, A., Kacarab, M., Wong, J. P. S., Small-Griswold, J. D., Thornhill, K. L., Noone, D., Podolske, J. R., Schmidt, K. S., Pilewskie, P., Chen, H., Cochrane, S. P., Sedlacek, A. J., Lang, T. J., Stith, E., Segal-Rozenhaimer, M., Ferrare, R. A., Burton, S. P., Hostetler, C. A., Diner, D. J., Seidel, F. C., Platnick, S. E., Myers, J. S., Meyer, K. G., Spangenberg, D. A., Maring, H., and Gao, L.: An overview of the ORACLES 500 (ObseRvations of Aerosols above CLouds and their intEractionS) project: aerosol–cloud–radiation interactions in the southeast Atlantic basin, *Atmos. Chem. Phys.*, 21, 1507–1563, <https://doi.org/10.5194/acp-21-1507-2021>, 2021.
- Scharffe, D., Slemr, F., Brenninkmeijer, C. A. M., and Zahn, A.: Carbon monoxide measurements onboard the CARIBIC passenger aircraft using UV resonance fluorescence, *Atmospheric Meas. Tech.*, 5, 1753–1760, <https://doi.org/10.5194/amt-5-1753-2012>, 2012.
- Schiller, C. L., Bozem, H., Gurk, C., Parchatka, U., Königstedt, R., Harris, G. W., Lelieveld, J., and Fischer, H.: 505 Applications of quantum cascade lasers for sensitive trace gas measurements of CO, CH₄, N₂O and HCHO, *Appl. Phys. B*, 92, 419–430, <https://doi.org/10.1007/s00340-008-3125-0>, 2008.
- St. Clair, J. M., Swanson, A. K., Bailey, S. A., and Hanisco, T. F.: CAFE: a new, improved nonresonant laser-induced fluorescence instrument for airborne in situ measurement of formaldehyde, *Atmospheric Meas. Tech.*, 12, 4581– 510 4590, <https://doi.org/10.5194/amt-12-4581-2019>, 2019.
- Tian, H., Xu, R., Canadell, J.G. *et al.* A comprehensive quantification of global nitrous oxide sources and sinks. *Nature* 586, 248–256 (2020). <https://doi.org/10.1038/s41586-020-2780-0>
- Viciani, S., Montori, A., Chiarugi, A., and D’Amato, F.: A Portable Quantum Cascade Laser Spectrometer for Atmospheric Measurements of Carbon Monoxide, *Sensors*, 18, 2380–2398, <https://doi.org/10.3390/s18072380>, 2018.
- 515 Zellweger, C., Steinbrecher, R., Laurent, O., Lee, H., Kim, S., Emmenegger, L., Steinbacher, M., and Buchmann, B.: Recent advances in measurement techniques for atmospheric carbon monoxide and nitrous oxide observations, *Atmospheric Meas. Tech.*, 12, 5863–5878, <https://doi.org/10.5194/amt-12-5863-2019>, 2019.